Program Digest, 2019 IEEE International Ultrasonics Symposium (IUS)
Glasgow, Scotland, October 6-9, 2019

Phase Aberration Correction in Transcranial Ultrasound Imaging using Averaged Sound Velocity Map in Delay-and-Sum Beamformer

Moein Mozaffarzadeh[1*], Claudio Minonzio[1], Martin D. Verweij[1,2],
Simone Hemm[3] and Verya Daeichin[1],
[1]Lab. of Acoustical Wavefield Imaging, Imaging Physics, Delft University of Technology, Delft, the Netherlands
[2]Dept. of Biomedical Engineering, Thorax Center, Erasmus MC, Rotterdam, the Netherlands
[3]Institute for Medical and Analytical Technologies, School of Life Sciences,
University of Applied Sciences and Arts Northwestern Switzerland FHNW, Muttenz, Switzerland
Email: M.Mozaffarzadeh@tudelft.nl

***Abstract*—Deep brain stimulation (DBS) is used to modify the brain function. Localization of the electrode(s) used in DBS is an important mater since the success of the treatment highly depends on it. Transcranial ultrasound imaging (TUI) can be a proper candidate to monitor the electrode(s), but it is affected by the phase aberration caused by the skull bone. To address this issue, in this paper, we propose a novel beamforming method based on the sound velocity map of the imaging medium. For each combination of the imaging grid and element of the array, an averaged sound speed (ASD) is calculated. Then, the ASD is used inside a delay-and-sum beamforming method. The numerical results show that the proposed method compensates the phase aberration caused by the skull having a thickness of 5 mm with a sound speed twice of the imaging medium (i.e., water). The proposed method can be implemented in a real-time manner, which makes it a great candidate to be used in operation rooms for surgeries.**

***Index Terms*—Transcranial ultrasound imaging, deep brain stimulation, adaptive beamforming, Phase compensation, aberration**

I. Introduction

In deep brain stimulation (DBS), an implanted electrode is used to locally stimulate the brain function [1], [2]. Accurate positioning of the electrode inside the brain highly affects the success of the treatment [3]. To monitor the electrode(s) positioning, transcranial ultrasound imaging (TUI) is a good candidate since it can be used as a real-time monitoring modality during the operation.

Currently, TUI is limited by the strong aberrating effect of the skull bone; it exhibits a high sound speed and density which leads to order(s) of magnitude larger attenuation and higher absorption, compared to normal tissues inside the head [4], [5]. Consequently, this aberrating effect leads to a shifted wavefront phase. On the other hand, most of beamformers used for image formation in ultrasound imaging utilize a constant sound speed [6], [7]. However, using a constant sound speed in TUI causes a phase error that deforms the images and makes the estimated location of the electrode unreliable.

* Corresponding author

The ability to non-invasively measure both the speed of sound in human skull and its thickness opens a possibility to correct the detected ultrasonic signals. In addition, by real-time adaptive beamforming methods, it would be possible to compensate the phase aberration in the reconstructed images. Using a dual-probe ultrasound imaging configuration to be placed on the opposing sides of the temporal bone, scattering and transmission data can be acquired to be used for phase abberation correction in TUI [8].

In this paper, we report on a novel method to overcome the aberration effect of the skull in transcranial USI. An average sound velocity map seen by each element of the array is calculated. Then, using an adaptive delay-and-sum (DAS) beamforming algorithm, the ultrasound images are reconstructed while the phase aberration caused by the skull is compensated. The proposed image reconstruction method is numerically evaluated and the results are promising.

This paper is organized as follows: Section II illustrates the proposed reconstruction method. The results along with a discussion are presented in section III. Finally, the conclusion is presented in section IV.

II. Beamforming

DAS beamforming algorithm is commonly used to form ultrasound images due to its simplicity and real-time implementation. DAS formula is as follows:

$$y_{DAS}(k) = \sum_{i=1}^{M} x_i(k - \Delta_{i,k}), \tag{1}$$

where $y_{DAS}(k)$ is the output of the beamformer, k is the time index, M is the number of elements of array, and $x_i(k)$ and $\Delta_{i,k}$ are the detected signals and the corresponding time delay for detector i and time index k, respectively [9]. $\Delta_{i,k}$ is calculated based on the distance between the location of the i^{th} element of the array and the focused point (indicated by the time index k):

$$\Delta_{i,k} = d_{i,k}/C, \tag{2}$$

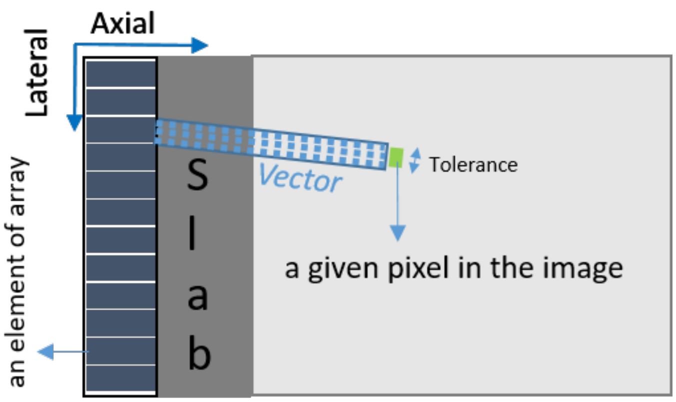

Fig. 1. The schematic of the grid-wise vector-based calculation of the necessary time delay used in the beamforming procedure (based on the sound velocity map).

where $d_{i,k}$ is the round-trip distance (between i^{th} element and the focused point), and C is the sound speed. Of note, the parameter $d_{i,k}$ should be indicated based on the imaging mode (plane wave, synthetic aperture, etc.).

Usually, a constant sound speed, C, is assumed (1480-1540 m/s) in the image reconstruction procedure [6], [7], [10]. As mentioned, in TUS, this assumption leads to an inaccurate image (affected by the phase aberration). In this paper, it is proposed to use an average sound velocity (C_{avg}) for each combination of a pixel in the image and an element of the transducer, instead of the constant sound speed (C). For simplicity, we only simulate (illustrated in section II) the effects of the sound speed of the human skull, and we ignore the sound speed variation between different tissues inside the head (see Fig. 1). Considering the sound speed of the skull (C_1) and the rest of the imaging medium (C), we propose to calculate the average sound velocity by the following equation

$$V_{avg}(j,k) = (LC_1C)\Big/\Big(Cx_{jk} + (L - x_{jk})C_1\Big), \qquad (3)$$

where j is the index of the element of the array, L is the number of the imaging grids (specified by $Tolerance$) existing in the vector which connects the j^{th} element to a pixel (see Fig. 1), and x_{jk} is the number of imaging grids having a sound velocity of C_1. It should be noticed that number of imaging grids having a sound velocity pf C_1, x_{jk}, is influenced by the element number, j, and imaging point, k.

III. Results and Discussion

To evaluate the performance of the proposed beamforming method, we used the k-Wave MATLAB toolbox [11]. The ground truth of the simulation is shown in Fig. 2. The imaging medium is extended 25 mm and 20 mm in the axial and lateral directions, respectively. A slab (mimicking the human skull), having a sound velocity of 3000 m/s and a thickness of 5 mm, covers the depth of 5-10 mm. A sound speed of 3000 m/s was chosen for the slab to emphasize the aberration effect. To simplify the numerical study, a point source of acoustic pressure is located at the depth of 17 mm, and the received signals at the depth of 0 mm are recorded using an ultrasound transducer array. 45 elements are used within the array, positioned at the depth of 0 mm, from -2.2 mm until 2.2 mm in the lateral direction. The array works at a central frequency of 6 Mhz and 77 % bandwidth. Noise is added to the detected signals (having a SNR of 50 dB) to have the numerical study close to experimental condition. In the reconstruction procedure, 512 $\times$ 512 pixels were used to form an image.

The reconstructed images using DAS with a constant sound speed (with/without) slab and DAS using a sound velocity map (proposed method) are shown in Figure 3. All the images are shown with a dynamic range of 45 dB; as seen in the colorbar. The Hilbert transform has been used to detect the envelope. Then, the final images are generated after normalization and log compression.

The Fig. 3(a) shows the formed image when there is no slab in front of the array. The target is correctly detected at the depth of 17 mm. In Fig. 3(b), in front of the array, there is a slab with a higher sound speed compared to the imaging medium (see Fig. 1(b)). Consequently, the acoustic source seems closer to the array (detected at a lower depth: 14.38 mm). Using the proposed method, it can be seen (in Fig. 3(c)) that the acoustic source is well-detected at its correct depth while the SNR is decreased.

To have the images evaluated in details, the axial variations of them are presented in Fig. 4 where the target is well-detected at the correct depth (where DAS (without any slab in front of the array) detects it). It also worth to mention that the corrected DAS leads to a lower range lobes compared to the DAS, with slab (see Fig. 4).

In this numerical study, we assumed the sound velocity map of the imaging medium as a known parameter. In practice, we can measure the speed of sound benefiting from Rayleigh-

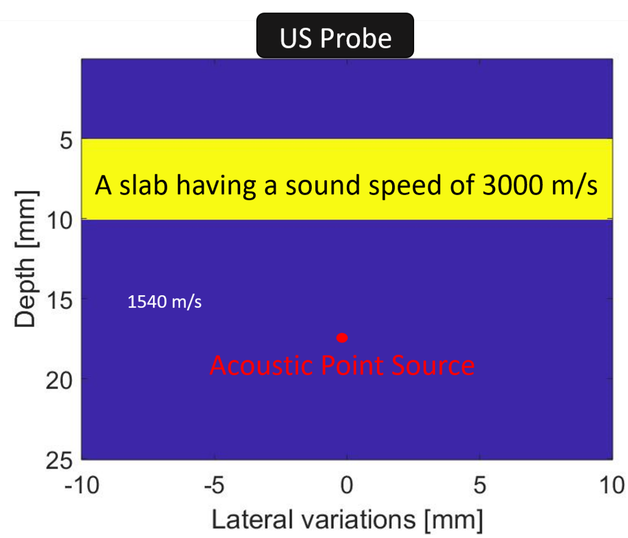

Fig. 2. The ground truth of the numerical study, showing the location of the acoustic point source and different sound speeds in the imaging medium.

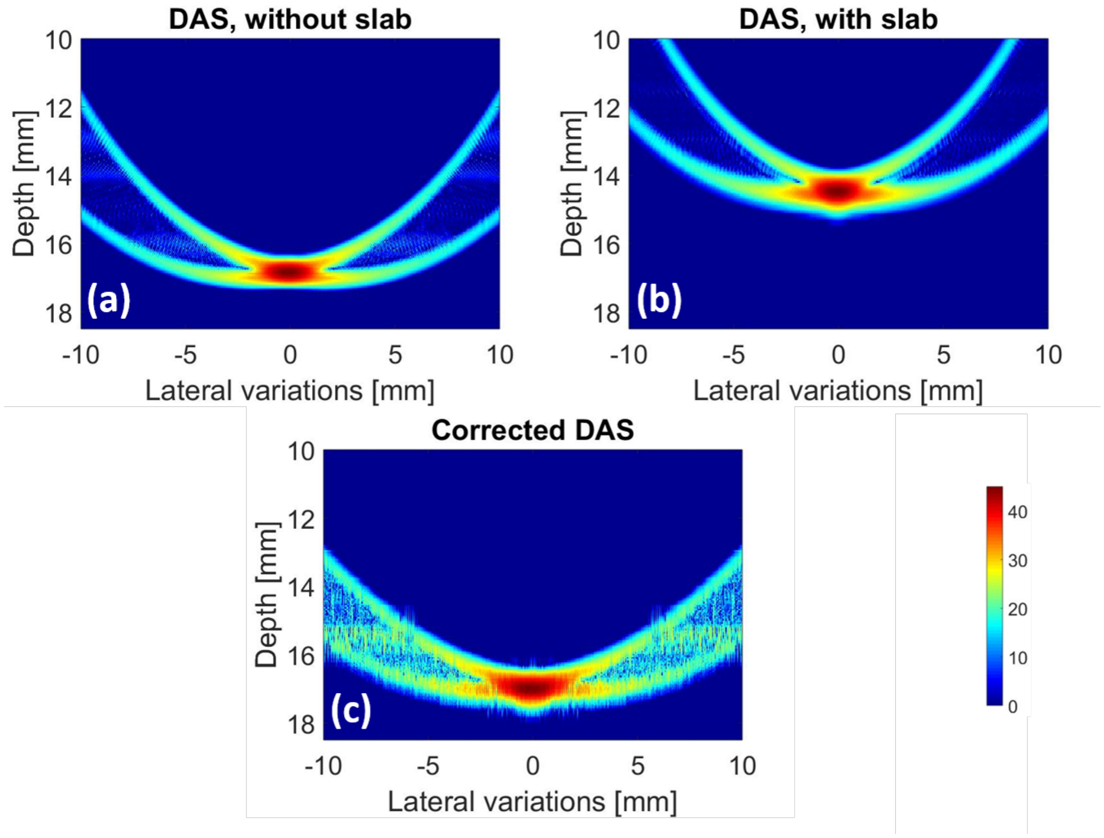

Fig. 3. The numerical images reconstructed by DAS where (a) no slab and (b) a slab is in front of the transducer. (c) The numerical images reconstructed by the proposed method (DAS using the corrected time delay). All the images are shown with a dynamic range of 45 dB.

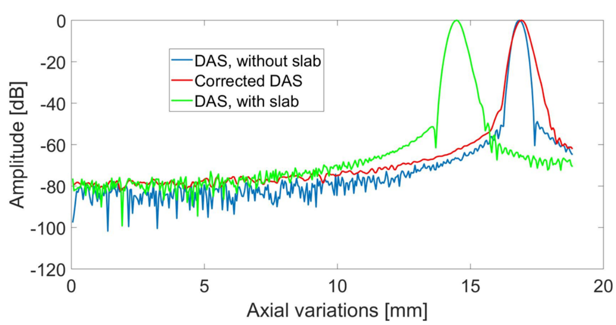

Fig. 4. The axial variation of the images presented in Fig. 3.

Lamb Waves generated when the medium is insonified with ultrasound waves. We can also use a pulse-echo method combined with the dual-probe imaging system to measure the thickness and sound speed of the skull.

Considering the benefits of the proposed method, We can use it in transcranial photoacoustic imaging (PAI) systems as well. PAI is based on the detection of the ultrasound waves generated by a laser irradiation [7], [10]. Therefore, the phase aberration also occurs when the laser induced acoustic waves go through the bone.

It took about 2 days to calculate the averaged sound speed maps (for an imaging medium of 256*256 pixels) using a PC having Intel(R) Xeon(R) Gold 6148 CPU @ 2.40 GHz and 64.0 GB RAM. This is due to the high number of combinations between the elements of the array and imaging medium. However, once the averaged sound velocity maps are generated, the proposed method can be implemented in a real-time manner. So, in practice, we only need to conduct a measurement of the patient a couple of days (depending on the number of imaging grids and array elements) before any surgery to have the averaged sound velocity maps ready by the time of the surgery.

As a future study, we will further evaluate the proposed beamforming method by experiments conducted with the dual-probe imaging system and a head phantom.

IV. Conclusion

localization of the electrode(s) used in DBS is a critical matter since the final results of DBS highly depends on it. TUI is a great candidate to do so, but it is affected by the phase aberration caused by the skull bone. To address this problem, we proposed an adaptive DAS beamforming method which uses the averaged sound velocity map of each combination of the imaging grid and array element. The proposed method was numerically evaluated considering an acoustic source at the depth of 17 mm propagating toward an ultrasound array through a skull having a thickness of 5 mm and a sound speed twice of the imaging medium (i.e., water). The results showed that the proposed method compensates the phase aberration and well detects the acoustic source at its correct depth. The greatest advantage of the proposed method (making it a great candidate for surgery guidance in operation rooms) is that it can be implemented in a real-time manner.

REFERENCES

[1] G. Deuschl, C. Schade-Brittinger, P. Krack, J. Volkmann, H. Schäfer, K. Bötzel, C. Daniels, A. Deutschländer, U. Dillmann, W. Eisner *et al.*, "A randomized trial of deep-brain stimulation for parkinson's disease," *New England Journal of Medicine*, vol. 355, no. 9, pp. 896–908, 2006.

[2] F. Alonso, D. Vogel, J. Johansson, K. Wårdell, and S. Hemm, "Electric field comparison between microelectrode recording and deep brain stimulation systemsa simulation study," *Brain sciences*, vol. 8, no. 2, p. 28, 2018.

[3] C. De Hemptinne, N. C. Swann, J. L. Ostrem, E. S. Ryapolova-Webb, M. San Luciano, N. B. Galifianakis, and P. A. Starr, "Therapeutic deep brain stimulation reduces cortical phase-amplitude coupling in parkinson's disease," *Nature neuroscience*, vol. 18, no. 5, p. 779, 2015.

[4] K. J. Haworth, J. B. Fowlkes, P. L. Carson, and O. D. Kripfgans, "Towards aberration correction of transcranial ultrasound using acoustic droplet vaporization," *Ultrasound in medicine & biology*, vol. 34, no. 3, pp. 435–445, 2008.

[5] K. Meyer-Wiethe, F. Sallustio, and R. Kern, "Diagnosis of intracerebral hemorrhage with transcranial ultrasound," *Cerebrovascular Diseases*, vol. 27, no. Suppl. 2, pp. 40–47, 2009.

[6] J.-F. Synnevag, A. Austeng, and S. Holm, "Benefits of minimum-variance beamforming in medical ultrasound imaging," *IEEE transactions on ultrasonics, ferroelectrics, and frequency control*, vol. 56, no. 9, pp. 1868–1879, 2009.

[7] M. Mozaffarzadeh, A. Mahloojifar, M. Orooji, S. Adabi, and M. Nasiriavanaki, "Double-stage delay multiply and sum beamforming algorithm: Application to linear-array photoacoustic imaging," *IEEE Transactions on Biomedical Engineering*, vol. 65, no. 1, pp. 31–42, 2018.

[8] F. Vignon, J. Aubry, M. Tanter, A. Margoum, and M. Fink, "Adaptive focusing for transcranial ultrasound imaging using dual arrays," *The Journal of the Acoustical Society of America*, vol. 120, no. 5, pp. 2737–2745, 2006.

[9] M. Mozaffarzadeh, M. Sadeghi, A. Mahloojifar, and M. Orooji, "Double-stage delay multiply and sum beamforming algorithm applied to ultrasound medical imaging," *Ultrasound in medicine & biology*, vol. 44, no. 3, pp. 677–686, 2018.

[10] M. Mozaffarzadeh, A. Mahloojifar, V. Periyasamy, M. Pramanik, and M. Orooji, "Eigenspace-based minimum variance combined with delay multiply and sum beamformer: Application to linear-array photoacoustic imaging," *IEEE Journal of Selected Topics in Quantum Electronics*, vol. 25, no. 1, pp. 1–8, 2018.

[11] B. E. Treeby and B. T. Cox, "k-wave: Matlab toolbox for the simulation and reconstruction of photoacoustic wave fields," *Journal of biomedical optics*, vol. 15, no. 2, p. 021314, 2010.